Jurnal Teknologi

Full Paper

THE EFFECT OF OXYGEN AND NITROGEN FUNCTIONAL GROUPS ON THE ELECTROCHEMICAL PERFORMANCE OF ORDERED CARBON

Nur Izzatie Hannah Razman[a*], Salasiah Endud[b], Izan Izwan Misnon[c]

[a]Centre of Foundation Studies, Universiti Teknologi MARA, Dengkil Campus, 43800 Dengkil, Selangor, Malaysia
[b]Department of Chemistry, Faculty of Science, Universiti Teknologi Malaysia, 81310 UTM Johor Bahru, Johor, Malaysia
[c]Nanostructured Renewable Energy Materials Laboratory, Faculty of Industrial Sciences & Technology, Universiti Malaysia Pahang, 26300 Kuantan, Pahang, Malaysia

Article history
Received
28 May 2018
Received in revised form
30 January 2019
Accepted
3 February 2019
Published online
18 April 2019

*Corresponding author
nurizz8627@puncakalam.uitm.edu.my

Graphical abstract

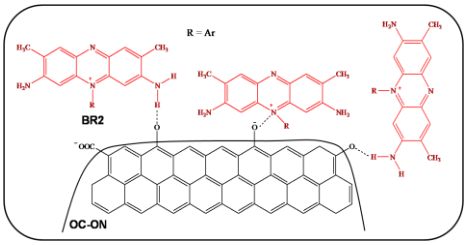

Abstract

Ordered carbon (OC) has been synthesised via replication strategy by using Santa Barbara Amorphous (SBA)-15 as a template. The successful replication process has been proven by nitrogen adsorption-desorption analyzer and transmission electron microscopy (TEM). The OC showed well-aligned mesopore system, similar to the SBA-15 template. The oxygen and nitrogen functional groups introduced were identified by X-ray photoelectron spectroscopy (XPS). Electrochemical performance of the oxygen containing OC (OC-O), nitrogen containing OC (OC-N), and oxygen nitrogen containing OC (OC-ON) was then evaluated by cyclic voltammetry (CV) and galvanostatic charge-discharge (GCD) using a three electrode system in 1M KOH aqueous electrolyte. The OC-O, OC-N, and OC-ON showed significant increment in specific capacitance, C_S and exhibited good capacitance retention (CR, %) over high scan rate and current density.

Keywords: SBA-15 template, ordered carbon, oxygen, nitrogen and electrochemical

Abstrak

Karbon bertertib (OC) telah disintesis malalui strategi replikasi dengan menggunakan Santa Barbara Amorphous (SBA)-15 sebagai templat. Kejayaan proses replikasi ini telah dibuktikan dengan penganalisis penjerapan-nyahjerapan nitrogen dan mikroskop pancaran elektron (TEM). OC menunjukkan sistem mesoliang sejajar yang baik, menyerupai templat SBA-15. Kumpulan berfungsi oksigen dan nitrogen telah dikenalpasti dengan spektroskopi fotoelektron sinar-X (XPS). Prestasi elektrokimia OC mengandungi oksigen (OC-O), OC mengandungi nitrogen (OC-N), dan OC mengandungi kedua-dua oksigen dan nitrogen (OC-ON) telah dinilai oleh voltammetri kitaran (CV) dan cas-nyahcas galvanostatik (GCD) menggunakan sistem tiga elektrod di dalam elektrolit akues 1 M KOH. OC-O, OC-N, dan OC-ON menunjukkan kenaikan kapasitan spesifik, C_S yang ketara dan ketahanan kapasitan (CR, %) yang baik pada kadar imbasan dan ketumpatan arus yang tinggi.

Kata kunci: SBA-15 templat, karbon bertertib, oksigen, nitrogen dan elektrokimia

1.0 INTRODUCTION

Ordered carbon (OC) is a material with a wide range of application. It has been used as adsorbent, supercapacitor, catalyst, and many more. Compared with other alternative carbon such as activated carbon, carbon nanofibers, and carbon nanotubes, OC offers more advantages because of its large specific surface area, high conductivity, and good chemical and environmental stability [1-3]. In 1990s, Ryoo *et al.* [4] introduced a preparation method of ordered structured carbon using porous silica as a template. This method is also known as replication strategy. The carbon replicate is uniformly porous with flexible pore size, providing interconnected channels for diffusion of electrochemically active species. Up to now, rapid development on the OC structures and properties has been reported.

In the study of electrochemical properties of carbon, researchers have found that oxygen functional groups have a great impact on the capacitive behaviour. Besides, oxygen functional groups can improve the hydrophilicity of carbon material which facilitates measurement involving aqueous media [5]. There has also been a similar discussion about nitrogen functional groups and its influence on carbon electrochemical properties. The nitrogen functional groups were able to induce additional pseudo-capacitance through faradaic redox reactions.

The oxygen and nitrogen groups can be introduced using various covalent and non covalent methods [5-8]. These methods alter the electronic structures of the carbon material, enhancing its surface polarity, electrical conductivity, electron-donor properties, and hydrophilicity [9]. However, only a few studies have reported the combined effect of oxygen and nitrogen functional groups on electrochemical performance of carbon materials [10-12].

In this study, OC was prepared *via* template replication strategy with Santa Barbara Amorphous-15 (SBA-15) as the template and sucrose as carbon precursor. The obtained OC was then modified by acidic oxidation to introduce oxygen functional groups (OC-O) and nitrogen-containing dye adsorption to introduce nitrogen functional groups (OC-N). A basic nitrogen-containing dye, Basic Red 2 (BR2) was used in order to modify the electrochemical activity of OC. Besides, the nitrogen containing species tend to attract water molecule making OC more hydrophilic. Both modification methods were also conducted to produce OC-ON in order to investigate the combined effect of both oxygen and nitrogen functional groups on OC. All four samples were electrochemically tested using cyclic voltammetry (CV) and galvanostatic charge–discharge (GCD) in 1 M KOH electrolyte, and to investigate the effect of oxygen and nitrogen functional groups on electrical capacitance of OC.

2.0 METHODOLOGY

2.1 Materials

The directing agent with a triblock copolymer structure, Pluronic 123 ($EO_{20}PO_{70}EO_{20}$ = 5800), tetraethyl orthosilicate (TEOS, silica source), and sucrose (carbon source) were purchased from Sigma Aldrich (Germany). The nitrogen functional groups were introduced using a basic dye, BR2 (C.I = 50240; Mol. wt. = 350.85 g mol^{-1}) obtained from Sigma-Aldrich (Germany). All other chemicals employed for material preparation and acidic oxidation were purchased from QReC™, Merck, Sigma-Aldrich, and RCI Labscan Ltd., and used without further purification. Distilled water was used to prepare all the solutions in this study. For electrochemical testing, polyvinylidene fluoride (PVDF) and carbon black (Super P, conductive) were obtained from Sigma-Aldrich (Germany) and Alfa Aesar (UK), respectively.

2.2 Preparation of Ordered Carbon, OC

Synthesis of SBA-15 template

SBA-15 was synthesised via the procedure reported by Zhao *et al*. [13] with some modifications. Pluronic P123 (4.0 g) was initially dissolved in 120 mL of 2 M HCl solution and 30 mL of water. TEOS (8.5 g) was then added to the solution and stirred at 35 °C for 20 hours. The mixture was aged at 80 °C for another 24 hours. Then, the solid product was recovered, washed, and dried at 60 °C. The Pluronic P123 surfactant was eliminated from the as-synthesised solid using a 200 mL Soxhlet extractor in ethanol–water mixture (50 wt.%) for 18 hours.

Synthesis of OC

OC was synthesised using sucrose as carbon source according to the procedure reported by Ryoo *et al*. [4]. Sucrose (1.25 g) was dissolved in H_2SO_4 solution, and 1.0 g of SBA-15 template was added to the solution. The homogeneous paste was heated up to 100 °C for 6 hours, followed by another 6 hours of heating at 160 °C. The product was again mixed with sucrose (0.8 g) and H_2SO_4 solution. The mixture was then heated as before. The final product was carbonised at 800 °C under an inert ambience for 1 hour. Finally, the carbon/SBA-15 composite was treated with 10 wt.% hydrofluoric acid (HF), washed, dried, and stored for further use.

OC Surface Modifications

Oxygen functional groups were introduced by acidic oxidation. A 0.1 g of OC was refluxed with 15 mL of 2 M HNO_3 solution at 80 °C for 2 hours. Then, the sample was filtered and dried. Besides, nitrogen functional groups were introduced by adsorption of BR2. A 50 mL of BR2 aqueous solution (200 mg L^{-1}) and 50 mg of OC were magnetically stirred in a

sealed 150 mL conical flask. Past 24 hours, OC solid was extracted from the adsorption vessel and fast filtered by using a syringe filter (nylon, hydrophobic, 0.45 µm). The collected solid was dried in a 60 °C oven.

2.3 Characterization of OC

Structural properties, such as surface area, pore volume, and pore size distribution, of SBA-15 template and OC were analysed by nitrogen adsorption–desorption isotherms at 77 K using a Micromeritics ASAP 2010 volumetric adsorption analyzer. All samples were outgassed at 130 °C for 12 hours prior to analysis. Specific surface areas were determined from Brunauer–Emmet–Teller (BET) plots, and pore size distributions were estimated by using the Barrett–Joyner–Halenda (BJH) method from the desorption branch. Transmission electron microscopy (TEM) was performed on a JEOL JEM-2001 electron microscope. Ground samples for TEM measurements were sonicated in ethanol for 2–5 minutes and then deposited onto a carbon-coated copper grid. The surface functional species of OC were determined using X-ray photoelectron spectroscopy (XPS; Kratos AXIS Ultra DLD; USA) in a vacuum of 2×10^{-9} mbar.

2.4 Electrochemical Measurement

The OC electrodes were prepared by mixing the samples (70 wt.%) with carbon (Super P, 15 wt.%) and PVDF binder (15 wt.%) using *N*-methyl pyrrolidinone as a solvent. The mixture was stirred for 24 hours and then coated onto a pre-cleaned nickel foam substrate. The coated electrode was heated in a 60 °C oven for 24 hours, and finally pressed at 5 Mpa using a hydraulic press. Cyclic voltammograms, CV were obtained in the potential range of –1.0 V to 0.0 V at various scan rates (10, 25, 50, 75, and 100 mV s^{-1}) using a three-electrode system equipped with a potentiostat (Autolab PGSTAT 30, Eco Chemie B.V., Netherlands). The gravimetric specific capacitance (C_S) was calculated using Equation 1:

$$C_S = \frac{1}{2mv(E_2 - E_1)} \int_{E_1}^{E_2} i(E)dE \quad (1)$$

where m, v, E_2, E_1, and i(E) are sample mass, scan rate, higher potential cut-off, lower potential cutoff, and current, respectively. Galvanostatic charge–discharge (GCD) curves were obtained by cycling the potential from –1.0 V to 0.0 V using 0.5, 1, 3, 5, and 7 A g^{-1} current densities. C_S was also calculated from the charge–discharge cycling tests using the Equation 2:

$$C_S = \frac{it}{m\Delta V} \quad (2)$$

3.0 RESULTS AND DISCUSSION

3.1 Characterisation of the Materials

The structural parameters of solid materials such as surface area and pore volumes can be evaluated from nitrogen adsorption-desorption analysis data. Table 1 shows specific surface area and pore volumes of SBA-15 template and OC. The specific surface area was calculated from BET multi-point analysis. Both SBA-15 and OC demonstrated high surface area SBET, similar to that reported by other studies [4, 7, 13] using the same method. SBA-15 template exhibited major fraction of mesopores (0.65 $cm^3\ g^{-1}$) and some micropores (0.05 $cm^3\ g^{-1}$). The OC exhibited 0.61 $cm^3\ g^{-1}$ mesopores and 0.32 $cm^3\ g^{-1}$ micropores.

Table 1 Structural parameters of the SBA-15 template and OC

Sample	[a] S_{BET} ($m^2\ g^{-1}$)	[b] V_{total} ($cm^3\ g^{-1}$)	[c] V_{meso} ($cm^3\ g^{-1}$)	[d] V_{micro} ($cm^3\ g^{-1}$)
SBA-15	498.20	0.70	0.65	0.05
OC	899.30	0.93	0.61	0.32

[a] Surface area determined from multi-point BET analysis.
[b] Pore volume at $P/P_o = 0.97$.
[c] From the difference between pore volume at $P/P_o = 0.97$ and V_{micro}.
[d] From *t* plot (Harkins–Jura equation).

Adsorption isotherms and pore size distribution of SBA-15 template and OC are illustrated in Figures 1 and 2, respectively. The isotherms of SBA-15 template and OC are type IV profile which is a characteristic of mesoporous materials. This characteristic is associated with capillary condensation in mesopores starts at a relative pressure (P/P_o) of about 0.40. The SBA-15 template exhibits a type H1 hysteresis loop associated with regular array of uniform spheres with a narrow pore size distribution. Meanwhile OC showed a type H3 hysteresis loop, which does not exhibit limiting adsorption at high relative pressure (P/P_o), and represents aggregates of carbon particles with slit shape pores [14]. The pore size distribution of the samples showed broad volume peaks centred at 4.5 nm and 4.0 nm for SBA-15 template and OC, respectively.

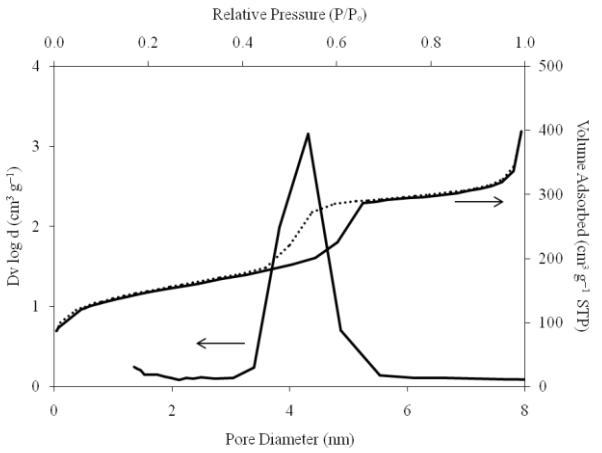

Figure 1 Adsorption-desorption isotherm and pore size distribution of SBA-15 template

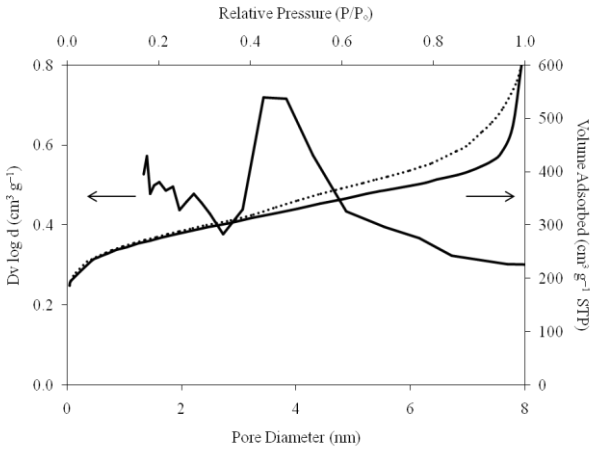

Figure 2 Adsorption-desorption isotherm and pore size distribution of OC

Porous materials are generally classified into three types, which are micropore (<2 nm), mesopore (2–50 nm), and macropore (>50 nm) [14, 15]. The microscopic image of the SBA-15 template (see Figure 3(a)) showed uniform align mesoporous system. The pores width estimated was 4.8 nm which lies in the range of mesopore category. In addition, the carbon replicate also showed systematic mesopores with size width approximately 4.8 nm (see Figure 3(b)). It is proved that both SBA-15 template and OC samples are composed of mesopore structures. These observations are consistent with the pore size distribution obtained from adsorption-desorption analysis data. Therefore, it can be concluded that the template replication strategy implemented in this study is successful.

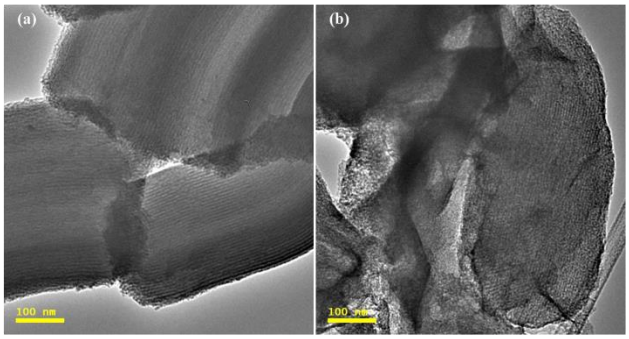

Figure 3 TEM images of (a) the SBA-15 template and (b) OC

The oxygen and nitrogen functional groups were identified using XPS. The main broad peaks in C 1s, O 1 s, and N 1s spectra were deconvulated (data not shown), and the atomic composition (%) are shown in Table 3. The composition of oxygen has increased from 8.0% to 13.7% after acidic oxidation. This finding proves that the acidic oxidation has successfully introduced several oxygen functional groups (C=O, –C–O, and quinone) on the surface of OC. Besides, nitrogen functional groups (pyridinic N and quaternary N) also present an increase in atomic composition from 0.3% to 2.0%. Both oxygen and nitrogen functional groups will later influence the electrical capacitance of OC [5, 6, 16, 17].

Table 2 Atomic percentage of carbon (C 1s), oxygen (O 1s), and nitrogen (N 1s) for OC and OC-O, OC-N, and OC-ON obtained through XPS analysis

Sample	Atomic Concentration (%)		
	C	O	N
OC	92.0	8.0	-
OC-O	86.0	13.7	0.3
OC-N	89.9	8.1	2.0
OC-ON	86.3	11.6	2.1

CV analyses were conducted at five different scan rates; 10, 25, 50, 75, and 100 mV s^{-1} in 1 M KOH electrolyte. CV profiles (see Figure 4) comprised a typical nearly rectangular shape with steep current change at the switching potential (–1.0 V and 0.0 V), which associated with electric double-layer capacitance behaviour.

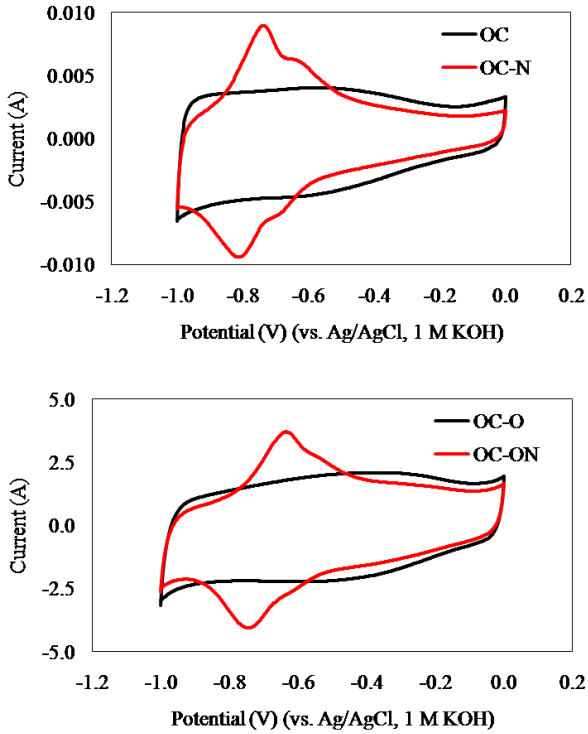

Figure 4 CV profiles of OC, OC-O, OC-N, and OC-ON samples at 10 mV s^{-1}

There were noticeable humps in the CV curves of OC-O and OC-ON, due to slow charging process induced by localisation of electrons on the inhomogeneous carbon surface [18]. The presence of oxygen functional groups has affected electronic resistance of the carbon materials [1, 19]. OC-O, OC-N, and OC-ON samples showed significant specific capacitance, C_S increment of 53.5%, 38.3%, and 57.8%, respectively. The increment in C_S occurred due to additional capacitance induced by oxidation and reduction reactions of oxygen and nitrogen functional groups. However, the C_S values of OC, OC-O, OC-N, and OC-ON decreased as the scan rates approached 100 mV s^{-1} but remained 89%, 78%, 96%, and 68% of their respective initial values. A decreased C_S at high scan rate may be owing to a partial detachment of carbon materials from the nickel foam substrate [20]. Even so, these results showed that all OC samples have relatively high C_S and good CR over high scan rates, even at low concentration of aqueous electrolyte. It is believed that other types of electrolyte such as organic or ionic liquid would promote higher C_S values.

The GCD measurements were conducted for 1000 cycles at various current densities (0.5, 1, 3, 5, and 7 A g^{-1}) in order to check the CR so that the samples can be used safely and steadily. CR values were calculated by comparing the initial and final values of obtained C_S. It is important to note that the value of capacitance obtained for OC was higher than activated carbon prepared from waste particle board and ordered mesoporous carbon [21, 22]. As can be seen in Table 3, the CR of OC is 79%, followed by OC-N (77%), OC-O (63%), and OC-ON (62%). The OC-O and OC-ON exhibited large deviate of CR value (16-17%) than the original OC associated with distributed-capacitance effect and impaired conductivity after HNO_3 oxidation [18]. The presence of oxygen functional groups had caused the conductivity of OC to reduce due to a decrease in the availability of delocalised π–electrons [23]. Besides, introduction of oxygen and nitrogen functional groups does affect the CR due to less ordered porosity which had caused difficulty for the KOH electrolyte ions to diffuse within the OC-O, OC-N, and OC-ON pores [2].

Table 3 Specific capacitance, C_S of OC, OC-O, OC-N, and OMC-ON at various scan rates (a) and current densities (b) and their capacitance retention, CR (%)

Sample	Specific Capacitance, C_S (F g^{-1})					
	a) Scan Rate (mV s^{-1})					
	10	25	50	75	100	[a] CR
OC	225.9	232.6	223.0	212.4	201.9	89.4
OC-O	346.7	342.7	319.3	295.6	270.3	78.0
OC-N	312.5	331.7	325.8	313.9	300.0	96.0
OC-ON	356.4	348.7	318.5	282.4	241.8	67.8
	b) Current Density (A g^{-1})					
	0.5	1	3	5	7	[a] CR
OC	147.3	142.0	126.8	120.2	116.3	79.0
OC-O	270.5	225.0	190.2	180.2	171.6	63.4
OC-N	160.2	144.4	129.9	125.7	123.3	77.0
OC-ON	278.0	226.2	190.4	180.1	172.4	62.0

[a] Capacitance retention, CR (%) = $\frac{C_{final}}{C_{initial}} \times 100\%$

4.0 CONCLUSION

In this study, oxygen and nitrogen functional groups have significantly improved the electrical performance of OC. At the scan rate of 10 mV s^{-1}, the C_S of OC-O, OC-N, and OC-ON demonstrated 53.5%, 38.3%, and 57.8%, respectively, increment compared to the original OC. Moreover, GCD tests performed at 0.5 A g^{-1} showed 83.6% (OC-O), 8.8% (OC-N), and 88.7% (OC-ON) capacitance increment. The increment relates to the additional capacitance induced by faradaic redox reactions of oxygen (–C=O, –C–O, and quinone) and nitrogen (pyridinic N and quaternary N) functional groups. These findings confirm that oxygen and nitrogen containing OC materials exhibited excellent feature for supercapacitor application.

Acknowledgement

The authors wish to acknowledge Ibnu Sina Institute for Fundamental Science Studies and University Industrial Laboratory, Universiti Teknologi Malaysia for the research facilities, Universiti Teknologi MARA for providing financial support through LESTARI grant

(600-IRMI/MyRA 5/3/LESTARI (075/2017)) and Amy Zuria Abdul Ajid (UTM) for XPS data analysis.

References

[1] Wu, X., Hong, X., Nan, J., Luo, Z., Zhang, Q., Li, L, Chen, H., and Hui, K. S. 2012. Electrochemical Double-layer Capacitor Performance of Novel Carbons Derived from SAPO Zeolite Templates. *Microporous and Mesoporous Materials*. 160: 25-31.

[2] Matsui, T., Tanaka, S., and Miyake, Y. 2013. Correlation between the Capacitor Performance and Pore Structure of Ordered Mesoporous Carbons. *Advanced Powder Technology*. 24: 737-742.

[3] Zhang, D., Hao, Y., Zheng, L., Ma, Y., Feng, H., and Luo, H. 2013. Nitrogen and Sulfur Co-doped Ordered Mesoporous Carbon with Enhanced Electrochemical Capacitance Performance. *Journal of Materials Chemistry A*. 1: 7584-7591.

[4] Ryoo, R., Joo, S. H., and Jun, S. 1999. Synthesis of Highly Ordered Carbon Molecular Sieves via Template-mediated Structural Transformation. *Journal of Physical Chemistry B*. 103(37): 7743-7746.

[5] Wu, X., Hong, X., Luo, Z., Hui, K. S., Chen, H., Wu, J., Hui, K. N., Li, L., Nan, J., and Zhang, Q. 2013. The Effects of Surface Modification on the Supercapacitive Behaviors of Novel Mesoporous Carbon Derived from Rod-Like Hydroxyapatite Template. *Electrochimica Acta*. 89: 400-406.

[6] Lang, J-W., Yan, X-B., Yuan, X-Y., Yang, J., and Xue Q-J. 2011. Study on the Electrochemical Properties of Cubic Ordered Mesoporous Carbon for Supercapacitors. *Journal of Power Sources*. 196: 10472-10478.

[7] Liu, F., Wang, J., Li, L., Shao, Y., Xu, Z., and Zheng, S. 2009. Adsorption of Direct Yellow 12 onto Ordered Mesoporous Carbon and Activated Carbon. *Journal of Chemical & Engineering Data*. 54: 3043-3050.

[8] Chen, H., Sun, F., Wang, J., Li, W., Qiao, W., Ling, L., and Long, D. (2013). Nitrogen Doping Effects on the Physical and Chemical Properties of Mesoporous Carbons. *Journal of Physical Chemistry C*. 117: 8318−8328.

[9] Koh, M. and Nakajima, T. 2000. Adsorption of Aromatic Compounds on CxN-Coated Activated Carbon. *Carbon*. 38: 1947-1954.

[10] Wang, H., Yu, W., Mao, N., Shi, J., and Liu, W. 2016. Effect of Surface Modification on High-Surface-Area Carbon Nanosheets Anode in Sodium Ion Battery. *Microporous and Mesoporous Materials*. 27: 1-8.

[11] Liu, H., Song, H., Chen, X., Zhang, S., Zhou, J., and Ma, Z. 2015. Effects of Nitrogen- and Oxygen-Containing Functional Groups of Activated Carbon Nanotubes on the Electrochemical Performance in Supercapacitors. *Journal of Power Sources*. 285: 303-309.

[12] Hulicova-Jurcakova, D., Seredych, M., Lu, G. Q., and Bandosz, J. T. 2009. Combined Effect of Nitrogen- and Oxygen-Containing Functional Groups of Microporous Activated Carbon on its Electrochemical Performance in Supercapacitors. *Advanced Functional Materials*. 19: 438-447.

[13] Zhao, D., Huo, Q., Feng, J., Chmelka, B. F., and Stucky, G. D. 1998. Nonionic Triblock and Star Diblock Copolymer and Oligomeric Surfactant Syntheses of Highly Ordered, Hydrothermally Stable, Mesoporous Silica Structures. *Journal of the American Chemical Society*. 120: 6024-6036.

[14] Sing, K. S. W., Everett, D. H., Haul, R. A. W., Moscou, L., Pierotti, R. A., Rouquerol, J., and Siemieniewska, T. 1985. Reporting Physisorption Data for Gas/Solid Systems with Special Reference to the Determination of Surface Area and Porosity. *Pure and Applied Chemistry*. 57: 603-619.

[15] Ryoo, R., Joo, S. H., Kruk, M., and Jaroniec, M. 2001. Ordered Mesoporous Carbons. *Advanced Materials*. 13(9): 677-681.

[16] Zhao, N., Wei, N., Li, J., Qiao, Z., Cui, J., and He, F. 2005. Surface Properties of Chemically Modified Activated Carbons for Adsorption Rate of Cr (VI). *Chemical Engineering Journal*. 115: 133-138.

[17] Xiao, Y., Cao, M., Ren, L., and Hu, C. 2012. Hierarchically Porous Germanium-Modified Carbon Materials with Enhanced Lithium Storage Performance. *Nanoscale*. 4: 7469-7474.

[18] Li, H., Xi, H., Zhu, S., Wen, Z., and Wang, R. 2006. Preparation, Structural Characterization, and Electrochemical Properties of Chemically Modified Mesoporous Carbon. *Microporous and Mesoporous Materials*. 96: 357-362.

[19] Fuertes, A. B., Pico, F., and Rojo, J. M. 2004. Influence of Pore Structure on Electric Double-Layer Capacitance of Template Mesoporous Carbons. *Journal of Power Sources*. 133: 329-336.

[20] Han, S. C., Kim, H. S., Song, M. -S., Kim, J. H., Ahn, H. J., and Lee, J. Y. 2003. Nickel Sulfide Synthesized by Ball Milling as an Attractive Cathode Material for Rechargeable Lithium Batteries. *Journal of Alloys and Compounds*. 351: 273-278.

[21] Wang, Z. and Zhang, L. 2013. Synthesis of Ordered Mesoporous Carbon and Their Electrochemical Performance. *Carbon*. 49: 4580-4588.

[22] Shang, T. W., Ren, R. Q., Zhu, Y. M., and Jin, X. J. 2015. Oxygen and Nitrogen-Co-Doped Activated Carbon from Waste Particleboard for Potential Application in High-Performance Capacitance. *Electrochimica Acta*. 163: 32-40.

[23] Jaramillo, M. M., Mendoza, A., Vaquero, S., Anderson, M., Palma, J., and Marcilla, R. 2012. Role of Textural Properties and Surface Functionalities of Selected Carbons on the Electrochemical Behaviour of Ionic Liquid Based-Supercapacitors. *RCS Advances*. 2: 8439-8446.